Improving shallow water MWD: Offshore Canada case study

Zheng Chang, Xuhui Luo, Jie Shu, Huifeng Zhu, CGG; Mervyn Parry, Kelly Kolb, Yvonne A Paisant-Allen, ExxonMobil Exploration Company

Summary

Data from towed streamer surveys in shallow water environments are usually contaminated by different orders of sea floor reflections called water-layer-related multiples (WLRMs). The model-based water-layer demultiple (MWD) method effectively removes WLRMs. The initial development of 2D MWD was followed by a 3D implementation to better handle out-of-plane WLRMs. This 3D implementation was further improved by using a selective-input strategy to handle the inconsistency of the high-frequency multiple patterns between adjacent sail lines and shots. Time-variant aperture scheme is proposed based on multiple contribution gathers (MCGs) to include sufficient large apertures, avoid aliasing problems, and compensate for apex shifting. Using narrow azimuth towed streamer (NATS) data from the Hibernia field, we demonstrate the benefit of selective-input MWD with time-variant apertures for attenuating WLRMs in shallow water data.

Introduction

Free-surface multiple attenuation is challenging for shallow water marine streamer data because of the lack of near offset information and the poor quality of water bottom primary reflections. The demultiple flow based on surface-related multiple elimination (SRME) (Verschuur et al., 1992) also suffers from cross-talk between different orders of multiples and from the wavelet distortion introduced by auto-convolution of the input data. MWD effectively attenuates WLRMs and thus is a good supplement to SRME for surface multiple attenuation in the shallow water environment (Wang et al., 2011, 2014). MWD predicts WLRMs (denoted by M) by convolving the Green's function, G, of the water layer with recorded data, D (Jin et al., 2012; Wang et al., 2011, 2014),

$$M(x_s, x_r) = \sum_{x_m \in \mathcal{M}_s} G(x_s, x_m) \otimes D(x_m, x_r) + \sum_{x_m \in \mathcal{M}_r} D(x_s, x_m) \otimes G(x_m, x_r), \quad (1)$$

where x_s, x_r, and x_m represent the source locations, receiver locations, and reflection points within the aperture ($\mathcal{M}_s$: source-side aperture; $\mathcal{M}_r$: receiver-side aperture) on the sea surface, respectively, and $\otimes$ represents the convolution operator. The first term in Equation 1 is the shot-side multiple, which includes reflections from the sea surface within the source-side aperture, $\mathcal{M}_s$, and the second term is the receiver-side multiple, which includes reflections from $\mathcal{M}_r$. MCGs are the traces obtained by convolving recorded data with the Green's function for the reflection points within the aperture prior to summation (Wang et al., 2011).

Depending on the surface locations x_m over which the summation is performed, we can either apply 2D MWD (Jin et al., 2012) or 3D MWD (Goss et al., 2013). With one-gun-one-cable input, 2D MWD effectively attenuates most WLRMs. However, it does not predict WLRMs associated with 3D effects. To address 3D out-of-plane multiples, MWD was extended to use common-offset cubes to predict 3D multiples. Hereafter, we call this original implementation of 3D MWD "regular 3D MWD".

Although regular 3D MWD provides better multiple models for out-of-plane multiples compared to 2D MWD, the mixture of data from different sail lines and shots in the common-offset cubes creates data inconsistency and thus degrades the multiple prediction at high frequencies. To overcome this issue and combine the benefits of 2D MWD with regular 3D MWD, Huang et al. (2015) proposed selective-input 3D MWD. Selective-input 3D MWD uses both regularized shot gathers from the same sail line and regularized common-offset cubes to predict WLRMs. When traces are needed for prediction of multiples, selective-input 3D MWD prioritizes traces from the regularized shot gathers over those from common-offset cubes. Using this approach, the predicted WLRMs are more consistent with those observed in the data at high frequencies while simultaneously including out-of-plane multiples.

We demonstrate that using a large aperture for MCG summation is beneficial for the prediction of low-frequency multiples. However, a large aperture can introduce aliasing noise into the MCG in the shallow area. In addition, the apexes of multiple events in MCG shift away from the midpoint towards the source/receiver locations as time increases. To address these problems, we propose a time-variant aperture scheme.

Using the Hibernia NATS survey, we demonstrate the need for a 3D algorithm to handle out-of-plane WLRMs. In addition, we demonstrate that selective-input 3D MWD with a time-variant aperture effectively handles both low- and high-frequency multiples better than earlier approaches.

Hibernia NATS data

The Hibernia oil field is located approximately 315 km east-southeast of St. John's, Newfoundland and Labrador,

DOI http://dx.doi.org/10.1190/segam2015-5906921.1

Canada. The water depth around Hibernia is approximately 70-90 m. The data for the study were acquired in 2001 using a shot interval of 18.75 m with flip/flop guns (i.e., 37.5 m per gun) and 8 streamers. The receiver interval for the survey was 12.5 m, and the streamer separation was 75 m. The streamer was towed at a fixed depth of 7 m below the sea surface. The shot and receiver configuration defined a natural bin grid of 6.25 x 18.75 m, a nominal fold of 60, and an offset range of 125-4800 m. Strong WLRMs overlaid the primaries in the reservoir zone, which made it challenging to accurately image this area.

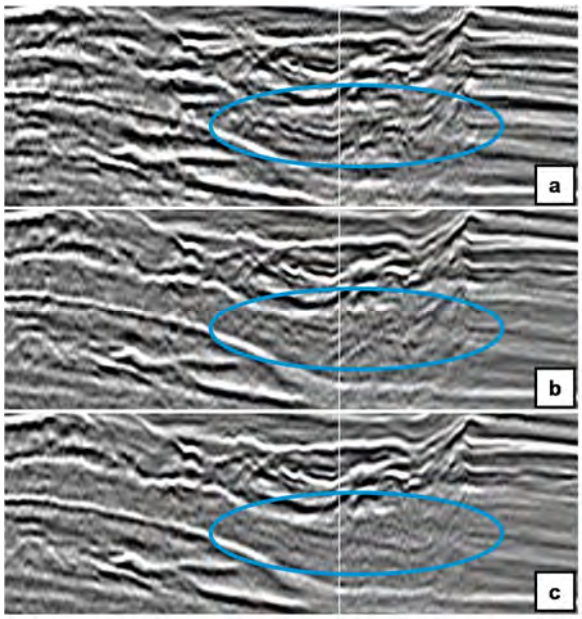

Figure 1: Hibernia post-stack time migration (a) before multiple removal, (b) after 2D model-based water-layer demultiple (MWD), and (c) after selective-input 3D MWD.

Limitations of 2D MWD

Historically, 2D MWD was applied to the Hibernia data. It effectively removed most of the WLRMs corresponding to the flat events. However, even though the geology in this area was relatively simple, there were still multiples with 3D effects that 2D MWD could not handle. We compared the results using selective-input 3D MWD with 2D MWD. A post-stack time migration (PoSTM) comparison of the results from 2D MWD and selective-input 3D MWD showed that 2D MWD left residual multiples of dipping events, while selective-input 3D MWD successfully attenuated them (Figure 1), indicating that the 3D approach performed better than 2D MWD. Identical curvelet-domain adaptive subtraction (Wu & Hung, 2013) parameters were used to isolate the improvement due to the different models.

Handling low-frequency multiple reverberations

To accurately predict low-frequency WLRMS, especially for peg-leg multiples from deep reflectors, the MWD apertures need to be sufficiently large. Given a discrete surface grid definition $\{x_m\}$, extremely large apertures may have artifacts associated with aliasing in the MCG as we move away from the apex. In shallow water, the apexes of the WLRMs MCGs shift from the midpoint towards the source/receiver locations as time increases. Figures 2a-2c show MCGs for a near channel trace located in the far cable with aliasing issues at the aperture edge for shallow events. Figure 2c shows that the apex was located around the midpoint along the crossline direction at early times and slowly moved towards the receiver location at large times (dashed line). We propose a time-variant aperture that is small in shallow areas and grows larger in deep areas to avoid aliased energy for shallow events while keeping the necessary aperture for low-frequency multiples of deep events. In addition, the time-variant aperture is more symmetric around the shifted apex in the shallow areas. Figures 2d-2f display the MCGs after applying the time-variant aperture scheme.

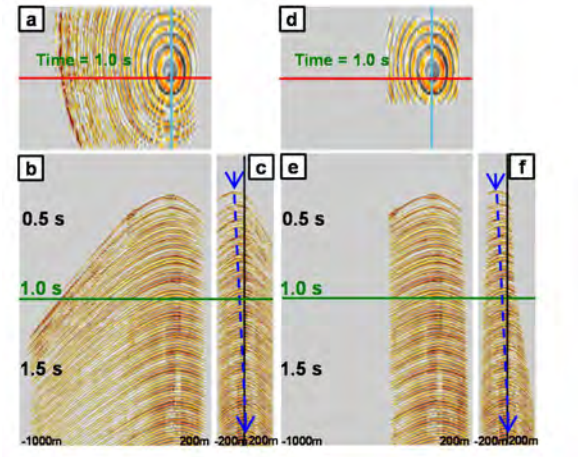

Figure 2: Receiver-side multiple contribution gather (MCG) for regular 3D MWD for a near channel at the far cable. Constant aperture: (a) time slice at 1000 ms. MCG section along the (b) inline direction and (c) crossline direction. Time-variant aperture: (d) time slice at 1000 ms. MCG section along the (e) inline direction and (f) crossline direction. The blue, red, and black lines indicate the location of the inline section, crossline section, and receiver, respectively, and the green line indicates the time for the time slice.

We compared brute stacks of regular 3D MWD output with three different apertures: constant small aperture, constant large aperture, and time-variant aperture. The time-variant aperture (Figure 3c) resulted in the best demultiple output. It removed more low-frequency multiples (deep blue arrow)

DOI http://dx.doi.org/10.1190/segam2015-5906921.1

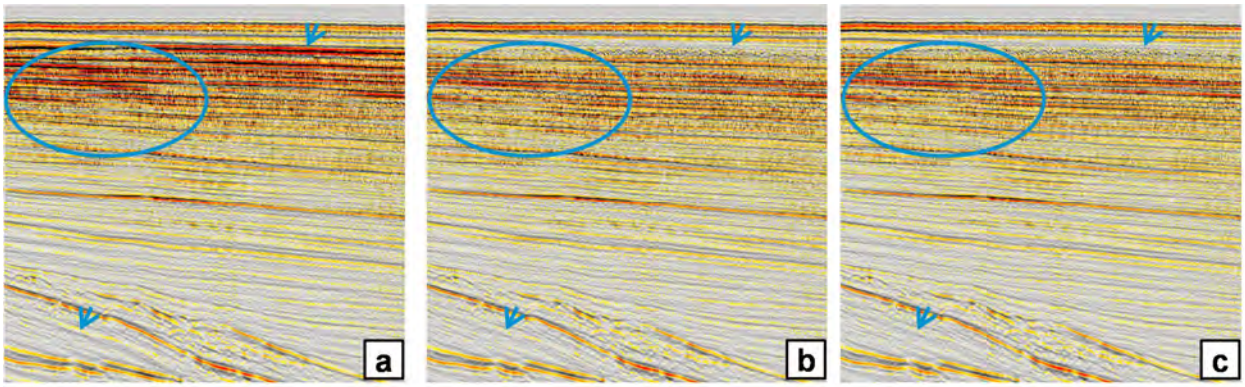

Figure 3: Brute stack of far cable demultiple output with (a) constant small aperture, (b) constant large aperture, and (c) time-variant aperture.

than the constant small aperture (Figure 3a) and had a cleaner shallow area (blue circle) compared to the constant large aperture (Figure 3b). Furthermore, by taking into account the apex shift, even though the effective aperture is small in the shallow, the demultiple output shows it can attenuate the first-order multiple (shallow blue arrow) as effectively as using a constant large aperture.

Handling high-frequency multiple reverberations

For shallow water surveys, it is extremely challenging to predict strong high-order water-layer reverberations with high frequencies. Even for sequences acquired close to each other in time and location, the high-order water-layer reverberations often show very different patterns. Figure 4a displays the acquisition position of two different shots from neighboring sequences that were acquired 13 hours apart. The sail lines were separated by only 285 m and covered overlapping midpoint locations, yet the multiple patterns, especially high-order multiple reverberations, were very different from each other (Figures 4b and 4e). These differences created challenges for model prediction using regular 3D MWD because these sequences were equally weighted and might be equal candidates for use in prediction. As a result, regular 3D MWD failed to accurately predict a multiple pattern similar to that in the input (Figures 4c and 4f). Selective-input 3D MWD, which prioritized traces in the same shots over those from common-offset cubes, predicted high-frequency multiples that better matched the input multiple pattern (Figures 4d and 4g).

To evaluate the impact on the final image, we adaptively subtracted both predicted models and migrated the results. Identical curvelet domain subtraction parameters were used for a fair comparison. The resulting 2D pre-stack depth migration stacks are shown in Figure 5. Figure 5a shows the input image before multiple attenuation. The demultiple output of regular 3D MWD (Figure 5b) left a significant amount of residual high-frequency multiples because of the mismatch of high-order multiple reverberations between the multiple model and input (Figure 4). The demultiple output of selective-input 3D MWD (Figure 5c) effectively removed those high-order multiple reverberations. An amplitude spectra comparison shows the same conclusion: the selective-input 3D MWD removed more high-frequency multiples compared to regular 3D MWD (Figure 5e). Figure 5d shows the difference between regular 3D MWD output and selective-input 3D MWD output.

Conclusion

We applied an improved shallow water MWD method to the Hibernia conventional NATS survey. We highlighted the limitations of 2D MWD and demonstrated how a 3D approach attenuates additional 3D multiples. We demonstrated that selective-input MWD with time-variant apertures better handles low-frequency multiples as well as high-order multiple reverberations. The time-variant aperture provides sufficient apertures to accommodate MCG apex shifting and discard aliased energy in MCGs. Compared to regular 3D MWD, the selective-input 3D MWD model better matched the input and resulted in a cleaner demultiple output, especially for the high-order multiple reverberations. While selective-input 3D MWD provides promising results, it is limited—as are 2D MWD, regular 3D MWD, and SRME—by the spatial sampling (e.g., shot density, smallest inline offset, largest crossline offset, and cable spacing.) and the signal-to-noise ratio of the acquired marine seismic data.

Acknowledgements

We thank the Hibernia co-venturers for permission to publish these results. We also thank Jiyang Wang for testing and Jeshurun Hembd, Sabaresan Mothi, and Yan

DOI http://dx.doi.org/10.1190/segam2015-5906921.1

Huang for their input. Special thanks go to Hui Huang, Ping Wang, and Shuming Hu for developing selective-input 3D MWD.

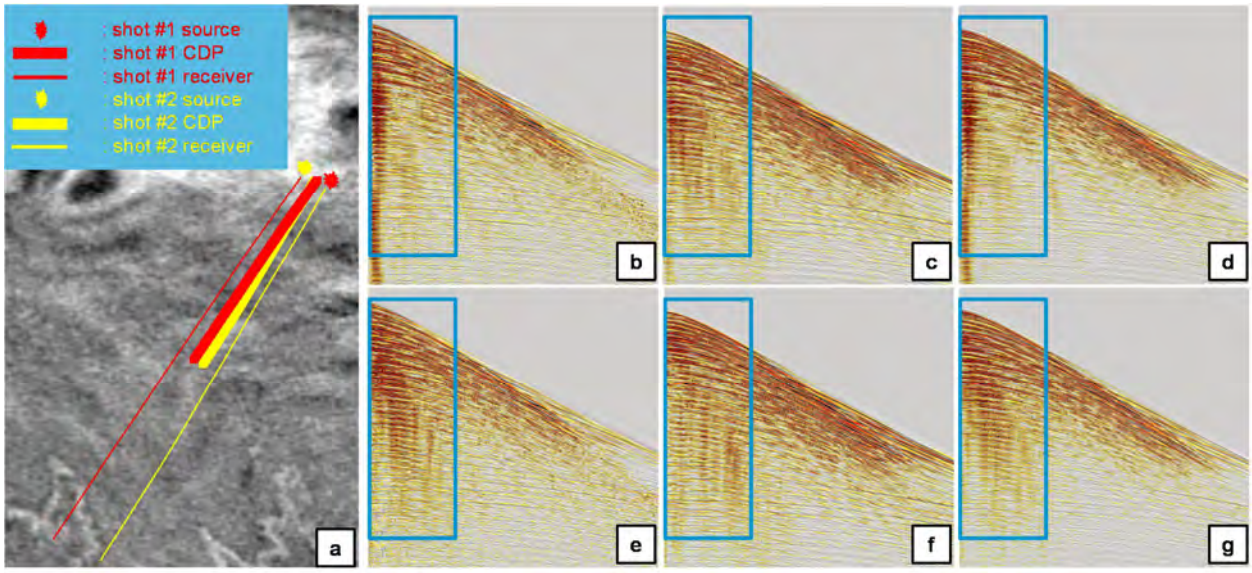

Figure 4: (a) Shooting position of Shot #1 and Shot #2. (b) Shot #1 MWD input. (c) Shot #1 regular 3D MWD model. (d) Shot #1 selective-input 3D MWD model. (e) Shot #2 MWD input. (f) Shot #2 regular 3D MWD model. (g) Shot #2 selective-input 3D MWD model.

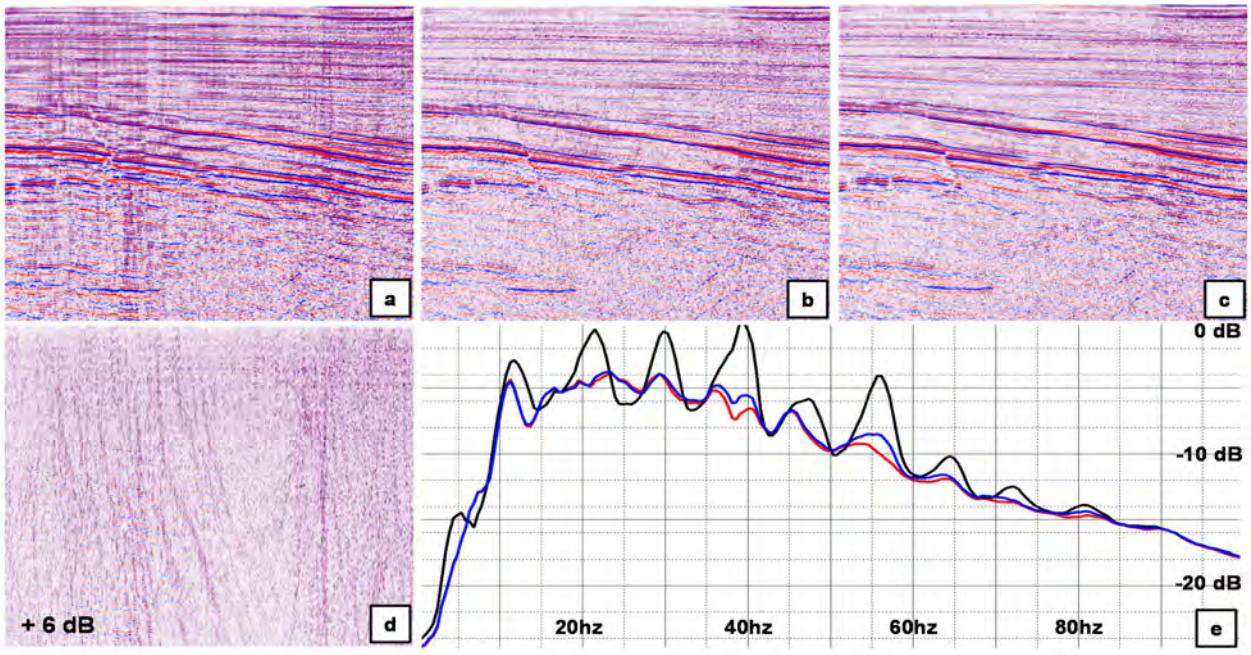

Figure 5: One-gun-one-cable pre-stack depth migration stretched to time (a) before multiple removal, (b) after demultiple output of regular 3D MWD, and (c) after demultiple output of selective-input 3D MWD. (d) Difference (with 6dB gain) between regular 3D MWD output and selective-input 3D MWD output. (e) Frequency spectra of input data (black), demultiple output of regular 3D MWD (blue), and demultiple output of selective-input 3D MWD (red).

DOI http://dx.doi.org/10.1190/segam2015-5906921.1

EDITED REFERENCES

Note: This reference list is a copyedited version of the reference list submitted by the author. Reference lists for the 2015 SEG Technical Program Expanded Abstracts have been copyedited so that references provided with the online metadata for each paper will achieve a high degree of linking to cited sources that appear on the Web.

REFERENCES

Goss, L. T., P. Wang, Z. Meng, N. Chazalnoel, C. Ting, S. Mothi, X. Meng, D. Maguire, and S. Knapp, 2013, Shallow water 3D MWD — A case study from West Africa: Presented at the 75th Annual International Conference and Exhibition, EAGE.

Huang, H., P. Wang, and S. Hu, 2015, Selective-input adaptation of model-based water-layer demultiple: Presented at the 77th Annual International Conference and Exhibition, EAGE.

Jin, H., M. Yang, P. Wang, Y. Huang, M. J. Parry, and Y. Paisant-Allen, 2012, Application of MWD for shallow water demultiple: Hibernia case study: Presented at the 74th Annual International Conference and Exhibition, EAGE.

Verschuur, D. J., A. J. Berkhout, and C. P. A. Wapenaar, 1992, Adaptive surface-related multiple elimination: Geophysics, **57**, 1166–1177. http://dx.doi.org/10.1190/1.1443330.

Wang, P., H. Jin, S. Xu, and Y. Zhang, 2011, Model-based water-later demultiple: 81st Annual International Meeting, SEG, Expanded Abstracts, 3551–3555.

Wang, P., H. Jin, M. Yang, and S. Xu, 2014, A model-based water-layer demultiple algorithm: First Break, **32**, no. 3, 63–68.

Wu, X., and B. Hung, 2013, High-fidelity adaptive curvelet domain primary-multiple separation: Presented at the 75th Annual International Conference and Exhibition, EAGE.

DOI http://dx.doi.org/10.1190/segam2015-5906921.1